

# Formation of Single-Chain Polymer Nanoparticles in Water through Host–Guest Interactions\*\*

Eric A. Appel, Joseph Dyson, Jesús del Barrio, Zarah Walsh, and Oren A. Scherman\*

The dynamic three-dimensional structures of enzymes are dictated by secondary bonding interactions and play a crucial role in both molecular recognition and allosteric regulation. Controlled crosslinking of single polymer chains in isolation, that can be seen as a mimic of the self-organization of enzymes, has previously been realized in organic solvents through crosslinking of multivalent polymer chains under highly dilute conditions.<sup>[1,2]</sup> In this instance, crosslinking must be specifically intramolecular to form these “self-collapsed” single-chain polymeric entities, which have been reported as discrete, spherical nanoparticle structures.<sup>[3–9]</sup> Whilst a few of the above systems are documented in the literature, where novel applications for such systems have been realized,<sup>[10,11]</sup> only a small number are shown to be reversible and only one example exists in water. Moreover, the controlled folding and unfolding of a single polymer chain in water has not yet been realized. A completely reversible form of this system would be beneficial for many reasons, especially in light of one notable property of these nanoparticles (NPs), which is their ability to produce non-Einsteinian reductions in viscosity.<sup>[12]</sup>

Supramolecular crosslinking motifs exploit well-established non-covalent interactions and their incorporation into molecular constructs has led to the formation of materials with novel properties.<sup>[13–17]</sup> Notable examples of such materials predominantly include gelating entities where intermolecular crosslinking leads to gel formation.<sup>[18]</sup> This strategy has been particularly successful for systems that consist of polymeric subunits which are able to gel through multivalent functionality.<sup>[19]</sup> Cucurbit[8]uril (CB[8]), a macrocyclic host molecule capable of binding two aromatic guest molecules simultaneously, is a suitable candidate for such reversible crosslinking on account of the variety of guests available for binding.<sup>[20]</sup> This allows for the use of guests with a range of orthogonal stimuli where guest binding can be controlled through simple external conditions (e.g. temperature, pH, light, competing guests), thus allowing for reversibility to be easily achieved. As a result, a variety of systems have already

been produced bearing this reversible CB[8]-based cross-linking motif.<sup>[21–23]</sup> Herein we document a CB[8]-mediated system for the preparation of metastable single-chain polymer nanoparticles. These nanoparticles are shown to form rapidly, are highly tunable and reversible and do not require protection chemistries (Figure 1).

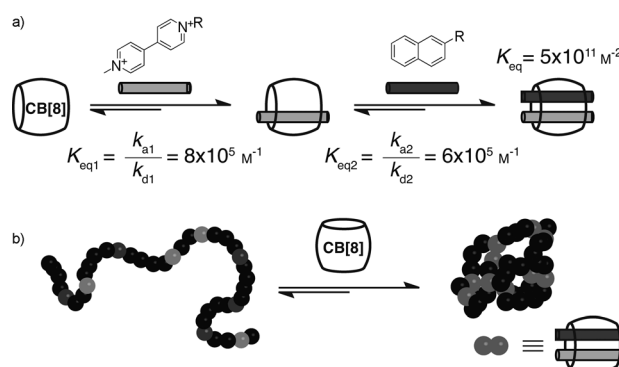


**Figure 1.** a) Ternary complex formation with CB[8] for first guest viologen (MV) and second guest naphthyl (Np) moieties and of b) collapse of single polymer chains by formation of a CB[8] ternary complex.

High molecular weight and water soluble poly(*N*-hydroxyethylacrylamide) precursors were synthesised using recent advancements in atom transfer radical polymerization (ATRP) of acrylamides (Table S1 in the Supporting Information).<sup>[24]</sup> The pendant hydroxyl functionality afforded by the polymer thus allowed for the conjugation of isocyanate functional guests for CB[8] to the polymer backbone in a random fashion (Figure 2).<sup>[25]</sup> Guest loadings were chosen in reference to previous work to observe significant variation in size and hydrodynamic volume upon polymer chain collapse.<sup>[4,5]</sup> Polymers were synthesized with either a 5 or 15% loading of each guest to observe the effect of different degrees of crosslinking on nanoparticle size. Proton nuclear magnetic resonance (<sup>1</sup>H NMR) spectroscopy confirmed the incorporation of the guests (Figure S1 in the Supporting Information), where clear signals for both viologen (MV) and naphthyl (Np) moieties are observed in the aromatic region. Moreover, an overlay of the UV/Vis and refractive index traces from gel permeation chromatography is observed for the functional polymer (Figure S1 in the Supporting Information).

Controlled intramolecular collapse of the functional polymer chains was achieved by stirring a solution of the polymer followed by addition of the crosslinker, CB[8]. Successful particle formation was observed at concentrations at or below 0.1 mg mL<sup>−1</sup> of polymer in solution. Monomodal

[\*] E. A. Appel, J. Dyson, Dr. J. del Barrio, Dr. Z. Walsh, Dr. O. A. Scherman  
Melville Laboratory for Polymer Synthesis  
Department of Chemistry, University of Cambridge  
Cambridge, CB2 1EW (UK)  
E-mail: oas23@cam.ac.uk

[\*\*] E.A.A. thanks Schlumberger for financial support and J.d.B is grateful for a Marie Curie Intraeuropean Fellowship (project number 273807). This work was also supported by an ERC Starting Investigator Grant (ASPIRe) and a Next Generation Fellowship provided by the Walters-Kundert Foundation.

Supporting information for this article is available on the WWW under <http://dx.doi.org/10.1002/anie.201108659>.

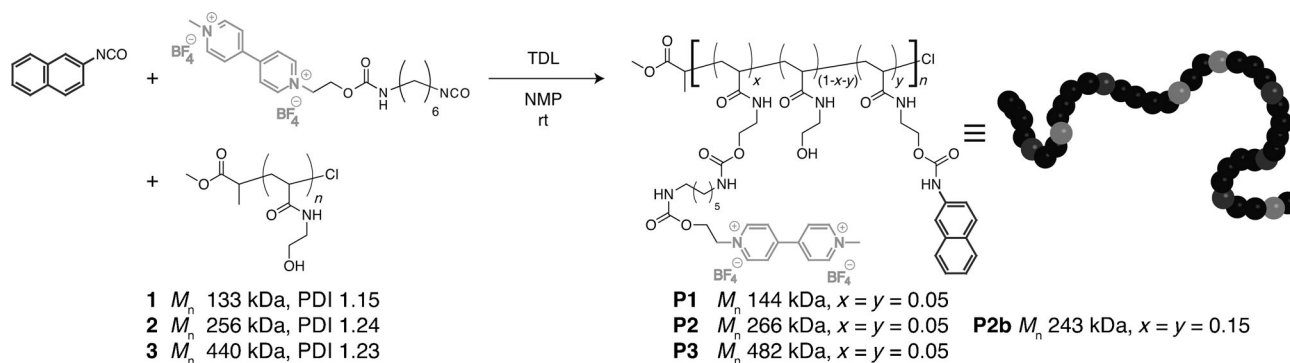


**Figure 2.** Facile isocyanate coupling reactions with both first and second guests simultaneously allow for near-quantitative functionalization of poly(*N*-hydroxyethyl acrylamide) homopolymers with relevant guests for CB[8] to be achieved (TDL = dibutyltin dilaurate, NMP = *N*-methylpyrrolidone, rt = room temperature).

distributions of polymer entities were observed using dynamic light scattering (DLS), along with a characteristic decrease in particle size upon collapse of the polymer chains. Higher polymer concentration or different order of addition yielded multimodal particle distributions which are attributed to the formation of multi-chain aggregates (see the Supporting Information).

Control experiments were performed whereby CB[7] was added to the polymer instead of CB[8]. The cavity of CB[7] is only large enough to encapsulate one guest (MV), therefore crosslinking and subsequent chain collapse cannot occur. In contrast to the addition of CB[8], an increase in the particle size was observed using DLS upon addition of CB[7].

To confirm that CB[8]-mediated, supramolecular crosslinking was occurring, UV/Vis and  $^1\text{H}$  NMR measurements were taken to directly compare the functional polymers and the characteristics of the analogous nanoparticles. Comparing polymer **P1** to its nanoparticle **NP1**, as a representative example, a downfield shift of peaks for the aromatic protons of Np, as well as those in the *meta* position relative to the cationic nitrogens of MV, in the  $^1\text{H}$  NMR spectrum showed that both aromatic guests are encapsulated in the CB[8] cavity (Figure S3 in the Supporting Information). In contrast, the aromatic protons in the *ortho* position relative to the cationic nitrogens of MV, being located in the electron-rich portal region of the CB[8] when complexed, demonstrated an upfield shift in the  $^1\text{H}$  NMR spectrum.<sup>[21]</sup> Moreover, the appearance of a peak at 521 nm in the UV/Vis spectra, correlating to a charge-transfer complex between the Np and MV moieties in the CB[8] ternary complex, strongly suggests that the desired crosslink is being formed.

DLS measurements confirmed the sizes for polymers **P1**–**P3** and their nanoparticle analogues **NP1**–**NP3** in solution, along with several control experiments (Figure 3 and Table S3 in the Supporting Information). From Figure 3a, both the polymers and the nanoparticles bear a molecular weight dependence. This trend is clear when considering increasing polymer chain lengths and hence hydrodynamic volume. Furthermore, size difference when undergoing collapse of the chains has a more pronounced effect as the molecular weight increases. Additionally, the polydispersities of the samples decrease upon collapse from the globular and disperse

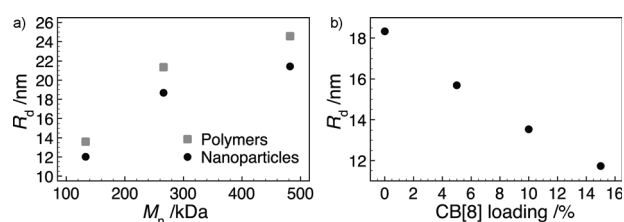


**Figure 3.** a) DLS measurements of functional polymers before and after addition of CB[8]. b) Titration of CB[8] to functional polymer **P2b** yields a linear decrease in the observed hydrodynamic diameter as the nanoparticle formed through ternary complexation becomes more tightly collapsed ( $M_n$  = molecular weight and  $R_d$  = hydrodynamic diameter).

polymeric state to the tightly collapsed nanoparticles (Table S3 in the Supporting Information). In contrast, the control experiment using CB[7] showed that addition of CB[7] yielded an increase in the particle size. This is likely on account of an increased bulk of the solvated chains with CB[7] complexing with the pendant MV guests.

The higher guest loading for **P2b** allowed for a titration of CB[8] to be made to directly monitor the particle size upon increasing the crosslinking (Figure 3b). The particle size of **NP2b** clearly decreased with increasing addition of CB[8] (Figure 3b) to a maximum crosslinking of 15 %, where the pendant guest moieties become saturated by CB[8]. These observations suggested that successful, quantitative crosslinking and subsequent chain collapse can be readily attained by addition of CB[8].

Atomic force microscopy (AFM) was used to determine whether there were morphological differences between the simple polymeric and CB[8]-formed particulate states, since three-dimensional data in fine detail is achievable at the appropriate size regime for the NPs. Figure 4 contains AFM images of highly dilute solutions of the nanoparticles (100 nm) which had been drop-cast onto mica, revealing that distinct particulate entities are clearly formed for all the nanoparticles (**NP1**–**NP3**). This provides direct support that CB[8] is successfully forming polymeric nanoparticles. This is further evidenced from control experiments which show that no particle formation was detected in the absence of CB[8] or in

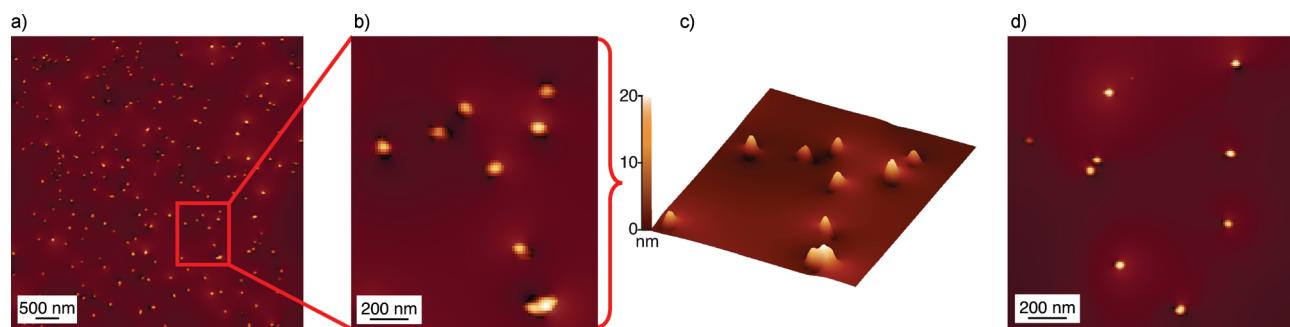


**Figure 4.** AFM imaging of single-chain polymeric nanoparticles. The various nanoparticles were drop-cast onto mica substrates: a) large scale image of **NP3**, b) zoom image of **NP3**, and c) three-dimensional image showing the spherical nature of the nanoparticles. d) **NP1**.

the presence of CB[7] (Figure S5 in the Supporting Information).

The kinetics governing nanoparticle formation provide valuable information about the rate and mechanism of folding and unfolding of the polymer chains, as well as further evidence that the nanoparticles are indeed formed from a single polymer chain. The reaction of CB[8] with the functional polymer to form the nanoparticles is a sequential, two-step process (Figure 1) and as the second step (the association of Np with the MV@CB[8] complex) is extremely fast,<sup>[19]</sup> the first step is rate-determining. The rate for the entire process can therefore be expressed according to a second-order rate equation [Eq. (S5) in the Supporting Information].<sup>[26]</sup>

Stopped-flow photophysical measurements were used to investigate the collapse kinetics of **NP2**, whereby the fluorescence of the polymer decreases on account of static quenching of the fluorescent Np moiety upon formation of the ternary complex crosslinks. Second-order rate constants  $k_{a1}$  and  $k_{d1}$  can be determined for the complexation of MV with CB[8] through systematic alteration of the concentration

of CB[8] in a large excess relative to the polymer chain whilst keeping the polymer concentration constant. Figure 5 displays the decrease in emission intensity with time observed upon addition of CB[8] to the polymer and quenching of the Np fluorescence and it is clear that the nanoparticles were completely formed within 0.5 seconds as a plateau in the fluorescence is reached. The kinetics curves were fit to a single exponential decay [Eq. (S1) in the Supporting Information] to give the observed rate constant,  $k_{obs}$ . The observed decay in emission intensity could potentially be related not only to static quenching upon complex formation, but also to dynamic quenching as the polymer chains begin to collapse into nanoparticles. However, the dynamic quenching was assumed to be negligible as the dependence of  $k_{obs}$  on the initial CB[8] concentration was linear (Figure 5, inset). The association and dissociation rate constants for the complexation of MV with CB[8] ( $k_{a1}$  and  $k_{d1}$ , respectively) were determined for the first time, according to Equation (S15) in the Supporting Information. The calculated value for the equilibrium constant ( $K_{eq1}$ ) compares with previous reports [Eqs. (1)–(3)].<sup>[27]</sup>

$$k_{a1} = (4.7 \pm 0.2) \times 10^5 \text{ M}^{-1} \text{ s}^{-1} \quad (1)$$

$$k_{d1} = (2.4 \pm 0.1) \text{ s}^{-1} \quad (2)$$

$$K_{eq1} = k_{a1}/k_{d1} = (2.0 \pm 0.1) \times 10^5 \text{ M}^{-1} \quad (3)$$

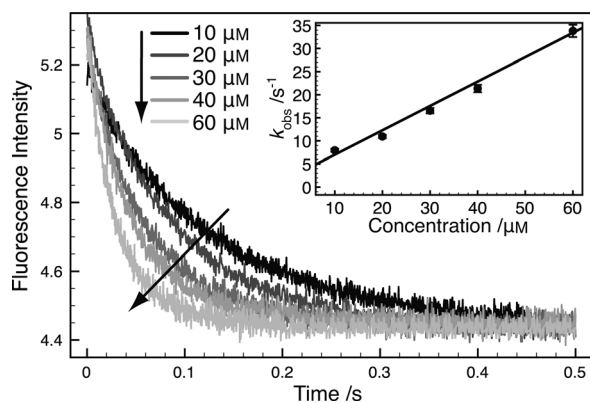


**Figure 5.** In situ monitoring of NP formation using stopped-flow photophysical measurements of the reaction of CB[8] with polymer **P2** demonstrating the decrease in fluorescence signal of the Np moiety upon binding with CB[8] and MV. The polymer concentration was kept constant at  $2.0 \mu\text{M}$  with respect to the Np moiety and the CB[8] concentrations range from  $10.0$ – $60.0 \mu\text{M}$ . The corresponding pseudo-first order plot demonstrating linearity in  $k_{obs}$  at various concentrations of CB[8] (inset). All concentrations indicated are the final ones after mixing.

Furthermore, a series of experiments was performed to probe the concentration dependence and stimuli-responsiveness of the equilibrium between the collapsed and expanded states of the nanoparticles (Figure 6). As a representative example, nanoparticle **NP2**, at different initial concentrations, was instantaneously diluted (10-fold) with both water and a solution containing an excess of 1-adamantanamine ( $\text{AdNH}_2$ ), which is a strongly competing guest for CB[8] ( $K_{eq} = 8 \times 10^8 \text{ M}^{-1}$ ),<sup>[28]</sup> and the fluorescence response monitored over time. To ensure dissociation of the ternary complex upon addition of the competing guest,  $\text{AdNH}_2$ , the concentration was made sufficiently high ( $1 \text{ mM}$ ) to overcome the effects of the high effective molarity ( $M_{eff}$ ) typically observed in intramolecular interactions.<sup>[29]</sup> Control experiments were developed whereby multi-chain aggregates were treated in the same manner as the single-chain nanoparticles **NP2**.

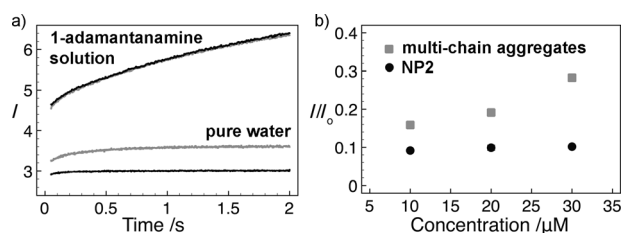


**Figure 6.** Dilution experiments using stopped-flow photophysical measurements of the instantaneous dilution of NP2 (black) and intermolecularly crosslinked polymer aggregates (grey). a) The response to dilution (10-fold) with water and with a 1.0 mM solution of 1-adamantanamine. Addition of 1-adamantanamine elicits an identical response from both the NPs and the multi-chain aggregates. b) Change in fluorescence with respect to the initial concentration of the polymeric particles.

These multi-chain aggregates were prepared from analogous polymers bearing only one type of guest, either MV or Np moieties (Figure S9 in the Supporting Information), thus exclusively containing intermolecular crosslinks which are inherently concentration dependent.

It is evident from Figure 6a that while both single-chain NPs and multi-chain aggregates exhibited the same response to the complete destruction of the ternary complex crosslinks by the  $\text{AdNH}_2$ , their response to dilution with water differs dramatically. This result indicated an important feature of the single-chain NP and multi-chain aggregate systems. Dynamic quenching of the Np fluorescence by the MV moiety upon dissociation of the ternary complex is either nonexistent in both systems or equivalent within the observed concentration range, no matter whether the MV and Np are bound to the same polymer chain or not. The dramatically different responses observed when diluted with water only were therefore primarily attributable to changes in the static quenching (Figure 6a).

The NPs containing intramolecular interactions within a single polymer chain are expected to be concentration independent, while the multi-chain aggregates formed through inherently intermolecular interactions are expected to be concentration dependent. The observed change in fluorescence ( $I/I_0$ ) verifies that the multi-chain polymer aggregates were indeed concentration dependent (Figure 6b). Dilution of the multi-chain aggregates caused disassociation of a portion of the ternary complex crosslinks and therefore liberation of fluorescent Np moieties, resulting in higher emission intensity than expected after a 10-fold dilution ( $I/I_0 > 0.10$ ). Additionally,  $I/I_0$  depended on the initial concentration of the aggregates and larger  $I/I_0$  were observed at higher initial concentrations. Each of these observations is consistent with theoretical predictions based on the intermolecular equilibrium binding constant for second guest binding,  $K_{eq2} = 1 \times 10^5 \text{ M}^{-1}$ , reported previously.<sup>[19]</sup>

In contrast, the observed decrease in fluorescence ( $I/I_0 \approx 0.10$ ) upon dilution of the NPs is commensurate with the 10-fold dilution, highlighting that they are concentration independent. This feature is consistent with the proposed intramolecular process, whereby the effect of a high  $M_{\text{eff}}$  allowed dilution to produce no observable effect on the degree of

crosslinking within the collapsed nanoparticles. This is clearly understood by looking again at the kinetic data for the formation of the NPs shown above (Figure 5). From this data it was possible to estimate the proportion of pendant moieties partaking in intramolecular crosslinking to be approximately 97% from the observed decrease in fluorescence emission of the Np moieties upon ternary complex formation. This value is far higher than that expected for purely intermolecular interactions at these concentrations (approximately 27%). Furthermore, assuming an intramolecular complexation process, an  $M_{\text{eff}}$  could be calculated from this degree of ternary complex formation to be approximately 3 mM, which is consistent with previous observations for various intramolecular processes.<sup>[29]</sup> Each of these observations corroborate those made with AFM and DLS and highly support our hypothesis that these NPs are formed by intramolecular interactions within a single polymer chain.<sup>[30]</sup>

In summary, a range of poly(*N*-hydroxyethylacrylamide) polymers were prepared by ATRP and were functionalized using an isocyanate conjugation method to incorporate both first and second guest moieties for complexation with CB[8]. These materials were subsequently “collapsed” at the molecular level in a supramolecular fashion using an intramolecular CB[8]-mediated crosslinking strategy in water. Well-controlled and defined structures, of which each entity has been shown to be due to the collapse of a single polymer chain, were successfully produced. Particle size in this instance can be easily tailored through simple addition of the crosslinking unit, CB[8], thereby allowing for a range of particle sizes to be easily accessed. Furthermore, the nanoparticle formation is exceptionally fast and completely reversible. The formation of these metastable nanoparticles, by virtue of the supramolecular nature of the intramolecular crosslinking within a single polymer chain in water, represents a major first step in developing synthetic polymers with aqueous phase behavior resembling that of their natural counterparts.

Received: December 8, 2011

Revised: February 20, 2012

Published online: March 15, 2012

**Keywords:** host–guest systems · kinetics · nanoparticles · polymers · supramolecular chemistry

- [1] D. Mecerreyes, V. Lee, C. Hawker, J. L. Hedrick, A. Wursch, W. Volksen, T. Magbitang, E. Huang, R. D. Miller, *Adv. Mater.* **2001**, *13*, 204–208.
- [2] E. Harth, B. Van Horn, V. Y. Lee, D. S. Germack, C. P. Gonzales, R. D. Miller, C. J. Hawker, *J. Am. Chem. Soc.* **2002**, *124*, 8653–8660.
- [3] A. Tuteja, M. E. Mackay, C. J. Hawker, B. van Horn, D. L. Ho, *J. Polym. Sci. Part B* **2006**, *44*, 1930–1947.
- [4] M. Seo, B. J. Beck, J. M. J. Paulausse, C. J. Hawker, S. Y. Kim, *Macromolecules* **2008**, *41*, 6413–6418.
- [5] E. J. Foster, E. B. Berda, E. W. Meijer, *J. Am. Chem. Soc.* **2009**, *131*, 6964–6966.
- [6] B. J. Beck, K. L. Killops, T. Kang, K. Sivanandan, A. Bayles, M. E. Mackay, K. L. Wooley, C. J. Hawker, *Macromolecules* **2009**, *42*, 5629–5635.



- [7] E. J. Foster, E. B. Berda, E. W. Meijer, *J. Polym. Sci.* **2011**, *49*, 118–126.
- [8] T. Mes, R. van der Weegen, A. R. A. Palmans, E. W. Meijer, *Angew. Chem.* **2011**, *123*, 5191–5195; *Angew. Chem. Int. Ed.* **2011**, *50*, 5085–5089.
- [9] A. Ruiz de Luzuriaga, I. Perez-Baena, S. Montes, I. Loinaz, I. Odriozola, I. Garcia, J. A. Pomposo, *Macromol. Symp.* **2010**, *296*, 303–310.
- [10] T. Terashima, T. Mes, T. F. A. De Greef, M. A. J. Gillissen, P. Besenius, A. R. A. Palmans, E. W. Meijer, *J. Am. Chem. Soc.* **2011**, *133*, 4742–4745.
- [11] M. Shokeen, E. D. Pressly, A. Hagooly, Z. A. N. Ramos, A. L. Fiamengo, M. J. Welch, C. J. Hawker, C. J. Anderson, *ACS Nano* **2011**, *5*, 738–747.
- [12] M. E. Mackay, T. T. Dao, A. Tuteja, D. L. Ho, B. van Horn, H.-C. Kim, C. J. Hawker, *Nat. Mater.* **2003**, *2*, 762–766.
- [13] B. J. B. Folmer, R. P. Sijbesma, R. M. Versteegen, J. A. J. van der Rijt, E. W. Meijer, *Adv. Mater.* **2000**, *12*, 874–878.
- [14] R. P. Sijbesma, F. H. Beijer, L. Brunsveld, B. J. B. Folmer, J. H. K. Ky Hirschberg, R. F. M. Lange, J. K. L. Lowe, E. W. Meijer, *Science* **1997**, *278*, 1601–1604.
- [15] A. Harada, R. Kobayashi, Y. Takashima, A. Hashidzume, H. Yamaguchi, *Nat. Chem.* **2011**, *3*, 34–37.
- [16] S. Burattini, B. W. Greenland, D. H. Merino, W. G. Weng, J. Seppala, H. M. Colquhoun, W. Hayes, M. E. Mackay, I. W. Hamley, S. J. Rowan, *J. Am. Chem. Soc.* **2010**, *132*, 12051–12058.
- [17] F. Wang, J. Q. Zhang, X. Ding, S. Y. Dong, M. Liu, B. Zheng, S. J. Li, L. Wu, Y. H. Yu, H. W. Gibson, F. H. Huang, *Angew. Chem.* **2010**, *122*, 1108–1112; *Angew. Chem. Int. Ed.* **2010**, *49*, 1090–1094.
- [18] B. J. Beck, S. J. Rowan, *J. Am. Chem. Soc.* **2003**, *125*, 13922–13923.
- [19] E. A. Appel, F. Biedermann, U. Rauwald, S. T. Jones, J. M. Zayed, O. A. Scherman, *J. Am. Chem. Soc.* **2010**, *132*, 14251–14260.
- [20] U. Rauwald, F. Biedermann, S. Deroo, C. V. Robinson, O. A. Scherman, *J. Phys. Chem. B* **2010**, *114*, 8606–8615.
- [21] U. Rauwald, O. A. Scherman, *Angew. Chem.* **2008**, *120*, 4014–4017; *Angew. Chem. Int. Ed.* **2008**, *47*, 3950–3953.
- [22] R. J. Coulston, S. T. Jones, T.-C. Lee, E. A. Appel, O. A. Scherman, *Chem. Commun.* **2011**, *47*, 164–166.
- [23] F. Tian, N. Cheng, N. Nouvel, J. Geng, O. A. Scherman, *Langmuir* **2010**, *26*, 5323–5328.
- [24] E. A. Appel, J. del Barrio, X. J. Loh, J. Dyson, O. A. Scherman, *J. Polym. Sci. Part A* **2012**, *50*, 181–186.
- [25] F. Biedermann, E. A. Appel, J. del Barrio, T. Gruending, C. Barner-Kowollik, O. A. Scherman, *Macromolecules* **2011**, *44*, 4828–4835.
- [26] Y. Jia, A. Kumar, S. S. Patel, *J. Biol. Chem.* **1996**, *271*, 30451–30458.
- [27] Ref. [20].
- [28] S. Liu, C. Ruspice, P. Mukhopadhyay, S. Chakrabarti, P. Y. Zavalij, L. Isaacs, *J. Am. Chem. Soc.* **2005**, *127*, 15959–15967.
- [29] C. A. Hunter, M. C. Misuraca, S. M. Turega, *J. Am. Chem. Soc.* **2011**, *133*, 582–594.
- [30] Although the NPs are almost entirely concentration independent, a very slight concentration dependence is observed, corresponding to 0.8% intermolecular crosslinking within the NPs at 10 mM. This identifies that a very small proportion of multi-chain particles are present at this concentration. Upon extrapolation, intermolecular crosslinking drops to below 0.02% at 100 nM, identifying that a negligible proportion of multi-chain particles are present. These observations verify that the NPs observed by AFM, prepared from 100 nM solutions, indeed consist of single polymer chains.